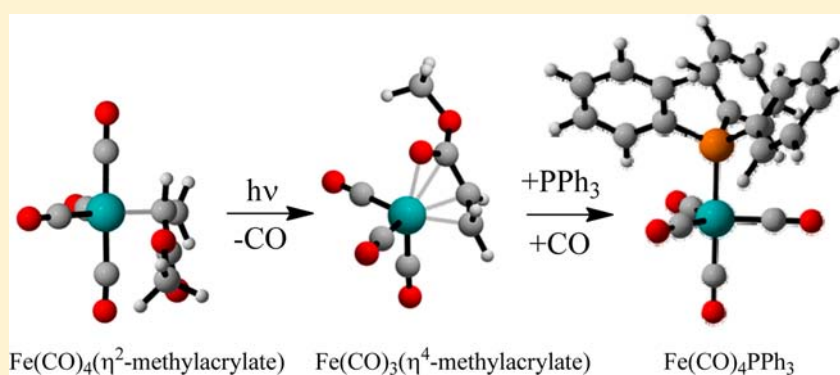# Light-Enhanced Displacement of Methyl Acrylate from Iron Carbonyl: Investigation of the Reactive Intermediate via Rapid-Scan Fourier Transform Infrared and Computational Studies

Sohail Muhammad,[†] Salvador Moncho,[†] Bo Li,[‡] Samuel J. Kyran,[‡] Edward N. Brothers,[†] Donald J. Darensbourg,*[,‡] and Ashfaq A. Bengali*[,†]

[†]Department of Chemistry, Texas A&M University at Qatar, Doha, Qatar

[‡]Department of Chemistry, Texas A&M University, 3255 TAMU, College Station, Texas 77843, United States

Ⓢ *Supporting Information*

$Fe(CO)_4(\eta^2\text{-methylacrylate})$ $Fe(CO)_3(\eta^4\text{-methylacrylate})$ $Fe(CO)_4PPh_3$

ABSTRACT: The thermal displacement of methyl acrylate from $Fe(CO)_4(\eta^2\text{-}CH_2=CHCOOMe)$ by phosphine ligands is a relatively slow reaction requiring several hours at elevated temperatures. In the present study, it is observed that photolysis of the tetracarbonyl complex with UV light activates the process such that the reaction is complete within a few seconds. This rate enhancement is due to the formation of an intermediate η^4 complex where the organic C=O and C=C units of methyl acrylate occupy axial and equatorial coordination sites on the Fe center, respectively, following photochemical CO loss. The displacement of methyl acrylate from this photolytically generated intermediate is facile with a remarkably low barrier of 8.7 kcal/mol. Density functional theory calculations support these experimental observations.

■ INTRODUCTION

It has long been known from the early work of Hoberg and Schaefer[1,2] that unsaturated nickel(0) complexes react with ethylene and CO_2 to afford nickelalactones. Recently, these derivatives have been shown to provide acrylates upon addition of methyl iodide[3] or tris(pentafluorophenyl)borane.[4] This is schematically represented in eq 1, where subsequent β-H

(1)
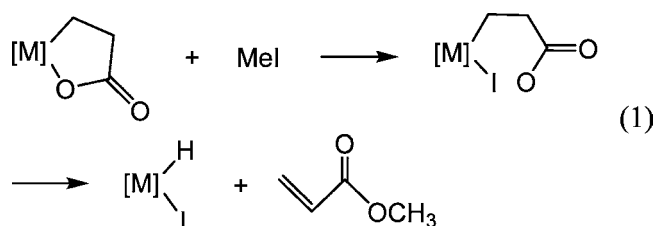
elimination leads to the production of methyl acrylate. An analogous process has also been reported with tetrakis-(trimethylphosphite)tungsten.[5] Hence, it is possible to envisage a sequence of reactions leading to a homogeneous catalytic

process transforming CO_2 into a value-added chemical via this approach.

In studies directed at expanding the scope of this chemistry to other metal complexes, we have characterized and investigated the reactivity of several acrylic acid derivatives of tetracarbonyl iron and ruthenium.[6] It was determined that thermal displacement of η^2-bound methyl acrylate by PPh_3 from ($\eta^2\text{-}CH_2=CHCOOMe)Fe(CO)_4$ (**1**) afforded both mono- and bisphosphine complexes with a half-life of greater than 5 h at 70 °C. Surprisingly, as described herein, this displacement reaction can be completed within seconds following photochemical activation of complex **1**. The reaction was found to proceed thermally from a transient complex, generated upon photolysis of **1**, in which methyl acrylate remains coordinated to the iron center.

Relevant to our study is the report in the mid-1970s by Koerner von Gustorf and co-workers,[7] where they examined the photochemical behavior of (η^2-methyl acrylate)$Fe(CO)_4$ in

the presence of excess methyl acrylate in hexane at −30 °C. The product of that reaction was identified by elemental analyses and mass, IR, and ^1H NMR spectroscopies as the bis(η^2-methyl acrylate) iron tricarbonyl (**2**). Upon warming a dilute solution of **2** to −5 °C, reversible loss of methyl acrylate readily occurred with the observation of a transient species proposed to have the structure **3**; that is, a 1-oxabutadiene complex with ν_{CO} bonds at 2064, 1994, and 1979 cm^{-1}.

3
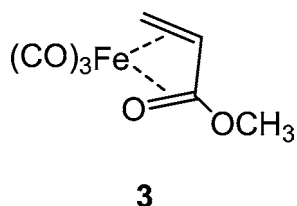
Presently, we report our observation of presumably the same transient complex (**3**) by rapid-scan infrared spectroscopy at room temperature produced by the photochemical loss of CO from complex **1**. Kinetic parameters for the displacement of the methyl acrylate ligand from the transient species have been determined. The results are supported by density functional theory (DFT) calculations which provide mechanistic insight into this unusual rate enhancement.

■ EXPERIMENTAL AND THEORETICAL METHODS

All experiments were conducted by use of a Bruker Vertex 80 FTIR operating in rapid-scan mode with a flow-through, temperature-controlled (±0.1 °C), 0.5 mm transmission cell with CaF$_2$ windows (Harrick Scientific). Sample photolysis was performed by use of the 355 nm output from a Nd:YAG laser (Continuum I-10). To avoid multiple photolysis events, a single shot of the laser was used to generate the time-dependent difference spectra. All spectra were obtained at 4 cm^{-1} resolution. In a typical kinetic run, a ≈ 1−2 mM heptane solution of **1** containing the required amount of PPh$_3$ prepared under a nitrogen atmosphere was flowed into the IR cell and the solution was allowed to thermally equilibrate for several minutes. The sample was then photolyzed, and spectral acquisition was initiated. The reactions were carried out over a 10-fold range of [PPh$_3$] and a 20 K temperature range. The observed rate constants (k_{obs}) were obtained from first-order exponential fits to the decay and growth of the reactant and product complexes, respectively. All solvents were of anhydrous grade and of >99% purity (Sigma−Aldrich). The Fe(CO)$_4$-(η^2-CH$_2$CHCOOMe) complex was synthesized according to literature.[6]

All calculations were performed in the Gaussian 09 suite of programs by use of density functional theory (DFT).[8] Energies, frequencies, and stationary point geometries were obtained by use of the ωB97XD functional[9] and the def2-TZVPP basis set.[10] While some elements in def2-TZVPP utilize effective core potentials, the elements considered in this study did not. The computed geometries were confirmed to be ground-state structures or transition states according to their number of imaginary frequencies. If not stated otherwise, the energies reported in the text are enthalpies computed at 298.15 K and 1 atm and are expressed in kilocalories per mole. Figures of computed geometries included in this work were rendered with CYLview.[11]

Infrared frequencies of carbonyl stretches were scaled by use of a linear fit to the value of the well-characterized species [i.e., Fe(CO)$_4$-(η^2-CH$_2$CHCOOMe), Fe(CO)$_4$PPh$_3$, Fe(CO)$_3$(PPh$_3$)$_2$, and CH$_2$CHCOOMe]. The calculated wavenumbers for the terminal CO ligands on the Fe center and the organic carbonyl in unligated methyl acrylate were fit to the experimental results. A linear fit to the equation $\nu^{calc} = 1.124\nu^{exp} − 121.97$, with a resulting correlation parameter of 0.997, was obtained.

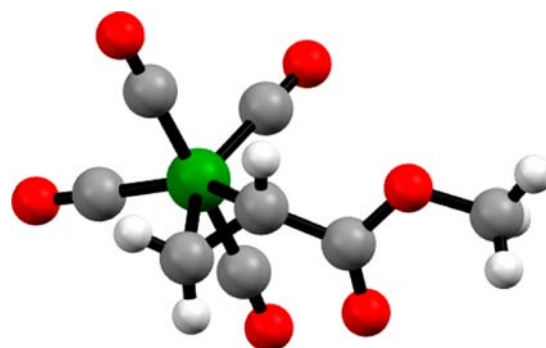**Figure 1.** Ball-and-stick representation of (CH$_2$=CHCOOMe)Fe(CO)$_4$ X-ray stucture.
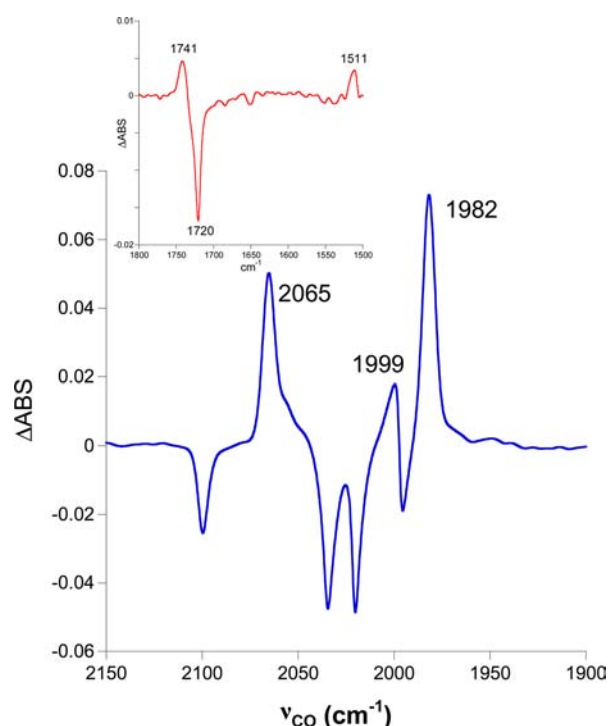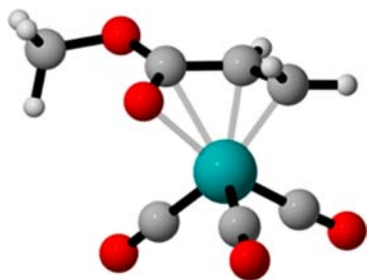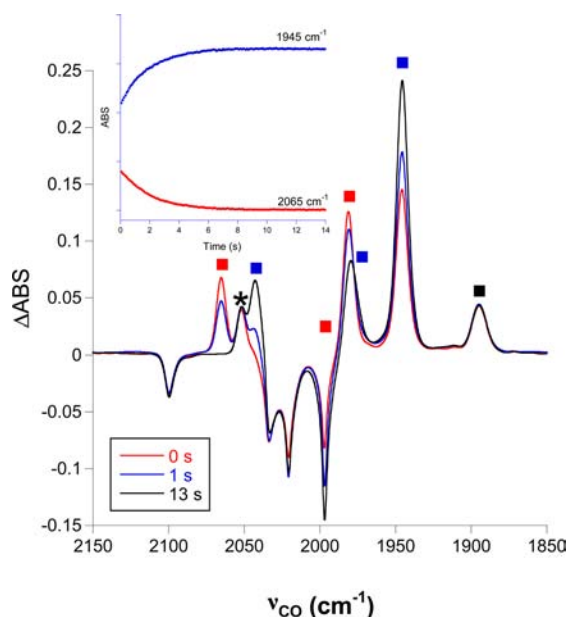

Figure 2. Difference FTIR spectrum obtained upon photolysis of **1** in heptane at 293 K. Negative peaks are due to destruction of parent, while positive peaks are due to complex **A**. (Inset) Peaks in the organic carbonyl region and are associated with the methyl acrylate ligand.

■ RESULTS AND DISCUSSION

Complex **1**, Fe(CO)$_4$(η^2-CH$_2$CHCOOMe), was prepared as previously described, and its determined X-ray defined structure is shown in the ball-and-stick drawing in Figure 1.[6] Photolysis of **1** in heptane solution at 293 K yields the difference Fourier transform infrared (FTIR) spectrum shown in Figure 2. The terminal CO bands due to the parent complex at 2100, 2033, 2020, and 1996 cm^{-1} decrease in intensity, along with the organic carbonyl stretch of the η^2-coordinated methyl acrylate at 1720 cm^{-1}. Subsequently, three new peaks corresponding to the terminal CO stretches of a new compound (**A**) are observed at 2065, 1999, and 1982 cm^{-1}. The position of these peaks correspond closely to the ν_{CO} bands previously assigned to **3**.[7] In addition, in the organic carbonyl region, peaks at 1741 and 1511 cm^{-1} are also observed. By comparison with a heptane solution of methyl acrylate, the former peak is associated with the free organic ligand generated upon photolysis of **1**.

Table 1. Experimental (Heptane) and Calculated CO Stretching Vibrations for Relevant Species

complex	ν_{CO} (cm^{-1})	
	exptl	calcd
Fe(CO)$_4$(η^2-CH$_2$CHCOOMe)	2100, 2033, 2020, 1996, 1720[a]	2081, 2036, 2019, 2004, 1713[a]
Fe(CO)$_4$PPh$_3$	2044, 1979, 1945	2040, 1984, 1953
Fe(CO)$_3$(PPh$_3$)$_2$	1895	1904
A	2065, 1999, 1982, 1511[a]	2055, 2008, 1998, 1523[a]
CH$_2$CHCOOMe	1740[a]	1734[a]

[a]Organic carbonyl.

Figure 3. Calculated structure of complex **A** generated upon photolysis of **1** in heptane solution.

Figure 4. Difference FTIR spectra obtained upon photolysis of **1** in the presence of 0.02 M PPh$_3$ in heptane at 283 K. Infrared bands are **A** (red, decay), Fe(CO)$_4$PPh$_3$ (blue, growth), and Fe(CO)$_3$(PPh$_3$)$_2$ (black). The 2052 cm^{-1} peak marked with an asterisk is unassigned. (Inset) Decay of **A** and growth of Fe(CO)$_4$PPh$_3$.

In light of DFT calculations discussed below, the weak peak at 1511 cm^{-1} is also assigned to complex **A** and provides important confirmation of the proposed structure. In the absence of added ligands, this species persists for a few minutes at room temperature. The experimental and calculated ν_{CO} values for the relevant complexes are presented in Table 1. The spectroscopic data guided by DFT calculations leads to the assignment of complex **A** as an η^4-coordinated Fe−methyl acrylate complex (Figure 3) in which the alkene and organic
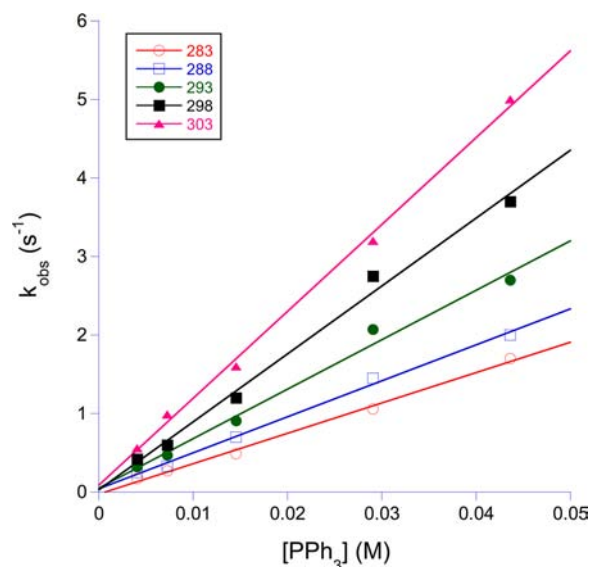
Figure 5. Plot of k_{obs} vs [PPh$_3$] for reaction of **A** with PPh$_3$ in heptane solvent at several temperatures.
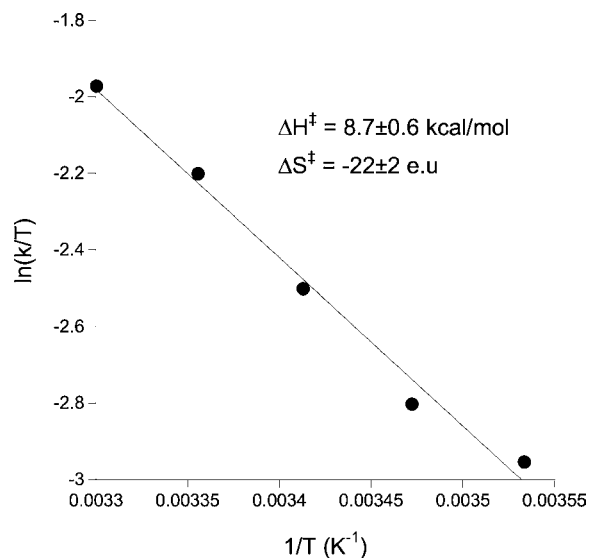
Figure 6. Eyring plot of second-order rate constants determined from the slope of the plots shown in Figure 5.

carbonyl occupy equatorial and axial coordination sites around the metal, respectively. This intermediate corresponds to complex **3** proposed by Koerner von Gustorf and co-workers.[7]

Photolytic loss of CO from metal carbonyls by UV light is a well-established phenomenon.[12] In the present case, loss of CO from **1** leads to a vacant coordination site and it is easy to envision a fast geometric reorganization of the already present η^2-coordinated methyl acrylate to yield an η^4 complex. The three CO bands observed are consistent with a tricarbonyl structure, although given the local C_{3v} symmetry, the peak at 1999 cm^{-1} has a lower-than-expected intensity since it overlaps with the bands of the depleted parent complex. The experimental terminal CO stretching vibrations are in good agreement with the calculated values for this geometry (Table 1). Several other geometries were modeled for this species but were found to be relatively unstable, including structures that placed the alkene in the axial position and ones that placed both alkene and organic carbonyl in the equatorial plane. Highly

Scheme 1
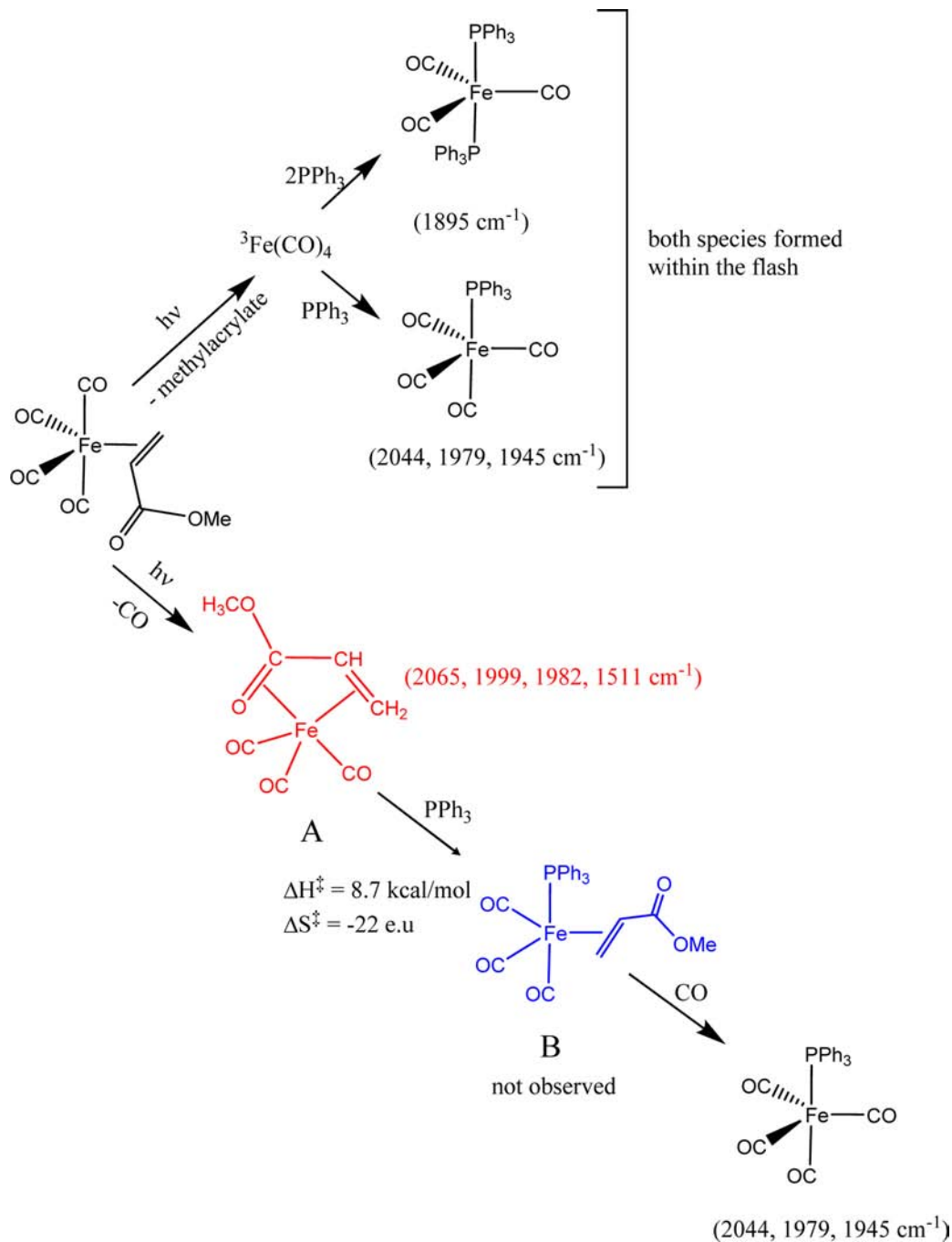
relevant is observation of the organic carbonyl stretching band that shifts from 1720 cm^{-1} in **1** to 1511 cm^{-1} when coordinated to the metal center in **A**. Of all the geometries modeled (including one where the ether rather than the carbonyl oxygen coordinates), the proposed structure is the only one that results in such a large shift. This ν_{CO} vibrational shift is in good agreement with the DFT calculated value and suggests that the interaction is between the metal center and the π electron density of the organic C=O bond rather than the terminal carbonyl oxygen.

Importantly, there is literature precedence for complexes such as **A** in the form of the η^4-coordinated enimine complex, Fe(CO)$_3$(CH$_3$CH=CH−CH=NC$_4$H$_9$), in which the C=C and C=N units occupy axial and equatorial coordination sites

around the Fe.[13] The CO bands of this complex (2060, 1998, and 1984 cm^{-1}) are within 5 wavenumbers of the species observed here. Furthermore, the 224 cm^{-1} shift in the C=N stretching vibration between the free and complexed ligands matches well with the 229 cm^{-1} shift observed in the C=O stretching vibration in the present case.

Photolysis of **1** in heptane solution in the presence of PPh$_3$, shown in Figure 4, results in the formation of **A**, Fe(CO)$_4$PPh$_3$ (2044, 1979, and 1945 cm^{-1}), and Fe(CO)$_3$(PPh$_3$)$_2$ (1895 cm^{-1}). An additional unassigned peak at 2052 cm^{-1} is observed that does not change in intensity as a function of time. A subsequent thermal reaction converts **A** to more Fe(CO)$_4$PPh$_3$ but not Fe(CO)$_4$(PPh$_3$)$_2$ within several seconds at room temperature. Previously, it was shown that in the analogous species,
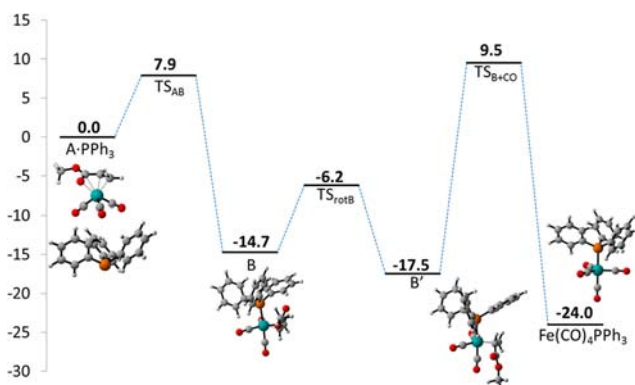
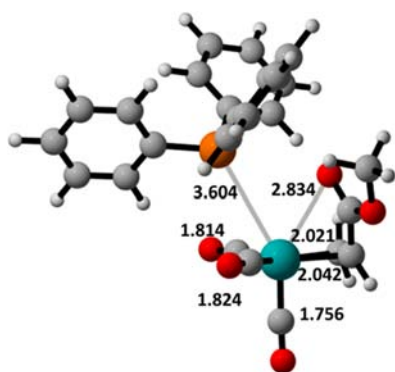**Figure 7.** Calculated enthalpic profile for reaction of **A** with PPh₃.

Figure 8. Calculated structure for TS$_{AB}$, which is consistent with associative attack of the PPh₃ ligand on **A**.

Fe(CO)₃(CH₃CH=CH−CH=NC₄H₉), the aliphatic enimine ligand was readily replaced by PPh₃.[13] Thus, in marked contrast to the thermal reactivity of **1**, the displacement of methyl acrylate by PPh₃ is complete within a few seconds of photolysis of **1** at ambient temperature.

As noted above, photolysis of **1** results in loss of either CO or methyl acrylate (evidenced by the presence of free methyl acrylate absorbing at 1740 cm⁻¹) to yield **A** and Fe(CO)₄, respectively.[7] Ultrafast IR studies coupled with DFT calculations have found that ³Fe(CO)₄ is the ground state of the tetracarbonyl and this species has been observed upon photolysis of Fe(CO)₄(η²-1-hexene).[14,15] These studies have also demonstrated that reaction of ³Fe(CO)₄ with PPh₃ results in the formation of both Fe(CO)₃(PPh₃)₂ and Fe(CO)₄PPh₃ within nanoseconds of CO loss. The current observation of both mono- and bisphosphine complexes immediately following the laser flash can therefore be readily accounted for.

A kinetic profile for the thermal reaction of **A** with PPh₃ was obtained. As shown in Figure 5, the observed rate constant, k_{obs}, varies linearly with [PPh₃]. Activation parameters of $\Delta H^{\ddagger} = 8.7 \pm 0.6$ kcal/mol and $\Delta S^{\ddagger} = -22 \pm 2$ eu, obtained from an Eyring analysis of the second-order rate constants (Figure 6), point to an associative process for the displacement of the η⁴-coordinated methyl acrylate from the iron center. It is therefore reasonable to suggest that this reaction involves displacement of the presumed weakly coordinated axial organic carbonyl in **A** by PPh₃ to yield an η²-alkene intermediate **B** and either subsequent or concerted displacement of the residual alkene bond by CO liberated upon photolysis. The overall reaction scheme is shown in Scheme 1.

The calculated enthalpic profile for the reaction shown in Figure 7 agrees partly with this proposed mechanism. Only the singlet surface was considered for the reactions since the triplet form of the starting complex **A** was found to be almost 13 kcal/mol less stable.

The calculated value of 7.9 kcal/mol for displacement of the organic carbonyl by PPh₃ to yield the alkene-coordinated η² complex (**B**) is in good agreement with the experimental estimate of 8.7 kcal/mol. The structure of the transition state, TS$_{AB}$, for this reaction is shown in Figure 8 and is consistent with an associative substitution mechanism. For example, the calculated enthalpy for a complex with a fully dissociated Fe−(C=O) bond is 10.6 kcal/mol higher than TS$_{AB}$, and the calculated 2.834 Å Fe−(C=O) distance in TS$_{AB}$ is intermediate between values of 2.088 Å for **A** and 3.747 Å for **B**.

The -CO₂Me group in **B** is pointed toward the axial PPh₃ ligand and has to rotate to form the stable isomer, which has it aligned with the axial CO, resulting in species **B′**.[16] However, contrary to the experimental evidence, a relatively high barrier is calculated for the reaction of **B′** with CO to yield Fe(CO)₄PPh₃. The most likely reason for this discrepancy is the fact that only static structures have been considered in the DFT studies. Rotation of the alkene ligand as the system proceeds from **B** to **B′** will involve the intermediacy of a complex in which the C=C bond is perpendicular to the equatorial plane. The structure for TS$_{rotB}$ (Supporting Information) is consistent with this assumption. Poor orbital overlap between the alkene moiety and the Fe(CO)₃PPh₃ fragment during this reorganization is expected to result in transient weakening of the Fe−alkene interaction. Supporting this suggestion are the calculated Fe−(C=C) bond distances, which are considerably longer in TS$_{rotB}$ (2.159 and 2.155 Å) relative to **B** (2.066 and 2.098 Å). It is therefore possible that the CO displaces methyl acrylate during this rotational process where the complex will not be in a resting-state geometry resulting in facile substitution. The static calculations reported here would fail to adequately capture such dynamic processes and may result in the inconsistency between theoretical and experimental findings.

■ CONCLUSIONS

While thermal displacement of η²-coordinated methyl acrylate from the Fe(CO)₄(η²-CH₂=CHCOOMe) complex by phosphines takes several hours at elevated temperatures, this reaction can be activated photolytically such that the reaction is complete within a few seconds at room temperature. The present study details the detection of a short-lived intermediate in the photolysis of Fe(CO)₄(η²-CH₂=CHCOOMe) by time-resolved FTIR spectroscopy, which undergoes rapid thermal reaction with PPh₃ to yield the monophosphine complex. Spectroscopic data together with DFT calculations help identify this intermediate as the Fe(CO)₃(η⁴-CH₂=CHCOOMe) species, in which the organic carbonyl and C=C unit of the methyl acrylate ligand bind to the axial and equatorial coordination sites of the Fe center, respectively. Light-enhanced displacement of CH₂=CHCOOMe from **1** by PPh₃ to form Fe(CO)₄PPh₃ proceeds with a remarkably low barrier of 8.7 kcal/mol, in dramatic contrast to the analogous thermal process, which has an enthalpic barrier of 31.7 kcal/mol.

■ ASSOCIATED CONTENT

ⓢ Supporting Information

One table of kinetic data, one figure with calculated structures, and all Cartesian coordinates for the modeled complexes.

This material is available free of charge via the Internet at http://pubs.acs.org.

■ AUTHOR INFORMATION

Corresponding Author

*E-mail djdarens@mail.chem.tamu.edu.

Notes

The authors declare no competing financial interest.

■ REFERENCES

(1) Hoberg, H.; Schaefer, D. *J. Organomet. Chem.* **1982**, *236*, C28.

(2) Hoberg, H.; Schaefer, D. *J. Organomet. Chem.* **1983**, *251*, C51.

(3) (a) Cokoja, M.; Bruckmeier, C.; Rieger, B.; Herrmann, W. A. *Angew. Chem., Int. Ed.* **2011**, *50*, 8510. (b) Lee, S. Y. T.; Cokoja, M.; Drees, M.; Li, Y.; Mink, J.; Herrmann, W. A.; Kuhn, F. E. *ChemSusChem* **2011**, *4*, 1275. (c) Bruckmeier, C.; Lehenmeier, M. W.; Relchandt, R.; Vagin, S.; Rieger, B. *Organometallics* **2010**, *29*, 2199.

(4) Jin, D.; Schmeier, T. J.; Williard, P. G.; Hazari, N.; Bernskoetter, W. H. *Organometallics* **2013**, *32*, 2152.

(5) Wolfe, J. M.; Bernskoetter, W. H. *Dalton Trans.* **2012**, *41*, 10763.

(6) Li, Bo.; Kyran, S. J.; Yeung, A. D.; Bengali, A. A.; Darensbourg, D. J. *Inorg. Chem.* **2013**, *52*, 5438.

(7) Grevels, F.-W.; Schulz, D.; Koerner von Gustorf, E. *Angew. Chem., Int. Ed.* **1974**, *13*, 534.

(8) Frisch, M. J.; Trucks, G. W.; Schlegel, H. B.; Scuseria, G. E.; Robb, M. A.; Cheeseman, J. R.; Scalmani, G.; Barone, V.; Mennucci, B.; Petersson, G. A.; Nakatsuji, H.; Caricato, M.; Li, X.; Hratchian, H. P.; Izmaylov, A. F.; Bloino, J.; Zheng, G.; Sonnenberg, J. L.; Hada, M.; Ehara, M.; Toyota, K.; Fukuda, R.; Hasegawa, J.; Ishida, M.; Nakajima, T.; Honda, Y.; Kitao, O.; Nakai, H.; Vreven, T.; Montgomery, J. A., Jr.; Peralta, J. E.; Ogliaro, F.; Bearpark, M.; Heyd, J. J.; Brothers, E.; Kudin, K. N.; Staroverov, V. N.; Kobayashi, R.; Normand, J.; Raghavachari, K.; Rendell, A.; Burant, J. C.; Iyengar, S. S.; Tomasi, J.; Cossi, M.; Rega, N.; Millam, J. M.; Klene, M.; Knox, J. E.; Cross, J. B.; Bakken, V.; Adamo, C.; Jaramillo, J.; Gomperts, R.; Stratmann, R. E.; Yazyev, O.; Austin, A. J.; Cammi, R.; Pomelli, C.; Ochterski, J. W.; Martin, R. L.; Morokuma, K.; Zakrzewski, V. G.; Voth, G. A.; Salvador, P.; Dannenberg, J. J.; Dapprich, S.; Daniels, A. D.; Farkas, Ö.; Foresman, J. B.; Ortiz, J. V.; Cioslowski, J.; Fox, D. J. *Gaussian 09, Revision B.01*; Gaussian, Inc., Wallingford, CT, 2009.

(9) Chai, J.-D.; Head-Gordon, M. *Phys. Chem. Chem. Phys.* **2008**, *10*, 6615−6620.

(10) Weigend, F.; Ahlrichs, R. *Phys . Chem. Chem. Phys.* **2005**, *7*, 3297−3305.

(11) Legault, C. Y. *CYLview, v 1.0b*; Université de Sherbrooke, 2009 (http://www.cylview.org).

(12) (a) Strohmeier, W. *Angew. Chem.* **1964**, *76*, 873. (b) Wrighton, M. *Chem. Rev.* **1974**, *74*, 401. (c) Bitterwolf, T. E. *J. Organomet. Chem.* **2004**, *689*, 3939.

(13) Otsuka, S.; Yoshida, T.; Nakamura, A. *Inorg. Chem.* **1967**, *6*, 20.

(14) Snee, P. T.; Payne, C. K.; Mebane, S. D.; Kotz, K. T.; Harris, C. B. *J. Am. Chem. Soc.* **2001**, *123*, 6909.

(15) Glascoe, E. A.; Sawyer, K. R.; Shanoski, J. E.; Harris, C. B. *J. Phys. Chem.* **2007**, *111*, 8789.

(16) Species B′ has previously been reported to be isolated and fully characterized. However, the ν_{CO} vibrational modes published are inconsistent with species B′, and the X-ray structure has not appeared in the open literature. See ref 7.